HHS Public Access

Author manuscript

Water Res. Author manuscript; available in PMC 2016 October 15.

Published in final edited form as:

Water Res. 2015 October 15; 83: 104–111. doi:10.1016/j.watres.2015.06.025.

In-situ Activation of Persulfate by Iron Filings and Degradation of 1,4-dioxane

Hua Zhong[a], **Mark L Brusseau**[*,a,b], **Yake Wang**[a], **Ni Yan**[b], **Lauren Quig**[c], and **Gwynn R Johnson**[c]

Hua Zhong: zhonghua@email.arizona.edu; Mark L Brusseau: brusseau@cals.arizona.edu; Yake Wang: yakew@email.arizona.edu; Ni Yan: niyan@email.arizona.edu; Lauren Quig: lquig@pdx.edu; Gwynn R Johnson: gjohnson@pdx.edu

[a]Soil, Water, and Environmental Science Department, School of Earth and Environmental Sciences, University of Arizona, Tucson, AZ 85721

[b]Hydrology and Water Resources Department, School of Earth and Environmental Sciences, University of Arizona, Tucson, AZ 85721

[c]Civil & Environmental Engineering, Maseeh College of Engineering & Computer Science, Portland State University, Portland, OR 97201

Abstract

Activation of persulfate by iron filings and subsequent degradation of 1,4-dioxane (dioxane) was studied in both batch-reactor and column systems to evaluate the potential of a persulfate-enhanced permeable reactive barrier (PRB) system for combined oxidative-reductive removal of organic contaminants from groundwater. In batch experiments, decomposition of persulfate to sulfate and degradation of dioxane both occurred rapidly in the presence of iron filings. Conversely, dioxane degradation by persulfate was considerably slower in the absence of iron filings. For the column experiments, decomposition and retardation of persulfate was observed for transport in the columns packed with iron filings, whereas no decomposition or retardation was observed for transport in columns packed with a reference quartz sand. Both sulfate production and dioxane degradation were observed for the iron-filings columns, but not for the sand column. The pH of the column effluent increased temporarily before persulfate breakthrough, and significant increases in both ferrous and ferric iron coincided with persulfate breakthrough. Multiple species of free radicals were produced from persulfate activation as determined by electron paramagnetic resonance (EPR) spectroscopy. The impact of the oxidation process on solution composition and iron-filings surface chemistry was examined using ICP-MS, SEM-EDS, and XRD analyses. A two-stage reaction mechanism is proposed to describe the oxidation process, consisting of a first stage of rapid, solution-based, radical-driven, decomposition of dioxane and a second stage governed by rate-limited surface reaction. The results of this study show successful persulfate activation using iron filings, and the potential to apply an enhanced PRB method for improving in-situ removal of organic contaminants from groundwater.

[*]Corresponding author: Brusseau@email.arizona.edu.

Keywords

persulfate; iron filings; dioxane; radical; surface reaction; permeable reactive barrier

1. INTRODUCTION

Contamination of groundwater by chlorinated-solvent constituents (e.g., trichloroethene, tetrachloroethene, carbon tetrachloride), 1,4-dioxane, and related compounds is ubiquitous, and remains a significant human-health and water-resource sustainability issue for many industrialized regions. Extensive dissolved-phase groundwater contaminant plumes typically form at sites contaminated by these compounds because of their relatively high aqueous solubilities (in comparison to regulatory standards), low retardation, and generally low (or very site dependent) transformation potential. These large plumes, which are typically hundreds of meters to several kilometers long, present complex and costly challenges to remediation and closure of the sites. In fact, it is now recognized that most sites with large groundwater plumes comprising these contaminants will require many decades or longer before cleanup will be achieved under current methods and standards (NRC, 2013). Hence, alternatives are under investigation for cost-effective, long-term management of sources and plumes at these sites.

One approach that has received widespread attention is the application of in-situ chemical oxidation (ISCO) for direct treatment. However, standard ISCO applications employing injection of aqueous solutions into a grid of wells are designed for relatively small areas, and are not cost-effective for treating large plumes. In addition, it is now recognized that most ISCO applications cannot fully treat the target area, thus leaving a residual source of contamination that must be managed. Another now-standard alternative for management of source zones and groundwater plumes is the use of permeable reactive barriers (PRBs). PRBs employing iron filings or related materials have been used successfully for many chlorinated-solvent contaminated sites, and have proven to be a cost-effective method for long-term management. However, standard PRBs are generally not effective for treating some of the primary contaminants of concern, such as dioxane, perfluoroalkyl compounds, or mixtures of such contaminants (Lee et al., 2012; EPA, 2006). We hypothesize that supplementing a standard iron-filings-based PRB with persulfate could significantly enhance the range of contaminants treated, as well as increase rates of treatment.

Activated persulfate is selected as the primary oxidant for our application based on the advantages of persulfate over other regularly used oxidants such as H_2O_2 and permanganate (Furman et al., 2010; Ahmad et al., 2010; Liang et al., 2003; Anipsitakis and Dionysiou, 2004; Huang et al., 2005; Nadim et al., 2006; Liang et al., 2007; Liang and Bruell, 2008; Lee et al., 2009; Rastogi et al., 2009; Guan et al., 2011; Fang et al., 2013a; Fang et al., 2013b). In general, persulfate activation refers to the use of energy or specific reagents to cause generation of the sulfate radical ($SO_4^{\bullet -}$) and/or hydroxyl radical ($HO^{\bullet -}$) in sufficient quantities for contaminant degradation. Common persulfate activation methods include heating (Lee et al., 2012; Liang, et al., 2003; Liang and Bruell, 2008; Ghauch et al., 2012; Johnson et al., 2008), UV irradiation, ultrasonication (Wang and Liang, 2014), electrochemical activation (Yuan and Liao, 2014), transition metal amendment (Liang and

Lee, 2008; Liang et al., 2004; Buxton et al., 1997), and base activation (Furman et al., 2010; Liang et al., 2007; Liang and Guo, 2012). Heat, base, and ferrous iron activation are the methods that are currently used for field ISCO applications (Block et al., 2004). Zero-valent iron (ZVI) has been shown to activate persulfate through release of Fe^{2+} into solution as the ZVI oxidizes (Lee et al., 2012; Lee et al., 2010). ZVI serves as a very capable activator not only because of the long-term supply capacity associated with its solid-phase form, but also due to an apparent synergistic interaction with persulfate (Lee et al., 2012; Lee et al., 2010; Oh et al., 2010). These results provide the basis for development of the persulfate-enhanced PRB (PE-PRB).

The objective of this study is to investigate the activation of persulfate by iron filings, and the resultant degradation of a representative generally recalcitrant organic contaminant (1,4-dioxane). Batch and miscible-displacement experiments were conducted to determine magnitudes and rates of degradation. Furthermore, the mechanisms for persulfate activation and dioxane degradation were explored by using SEM-EDS, XRD, and ICP-MS to characterize solid and aqueous phase geochemistry, while free-radical formation was measured using EPR spectroscopy.

2. MATERIALS AND METHODS

2.1. Materials and Chemicals

Iron filings (lab grade, Ward's Science, Rochester, NY), sieved (45-mesh) to exclude the ≤ 355 μm size fraction, were used in batch and column experiments. Compositional analysis of these iron filings was conducted using X-ray diffraction (XRD, X'Pert Pro MPD, PANalytical, Almelo, Netherlands) and variable pressure SEM (S-3400N) equipped with an energy dispersive X-ray spectrometer (UltraDry EDS, Thermo Scientific, Madison, WI). Commercially available natural silica sand (40/50 mesh Accusand, Unimin Corporation) was used to represent a natural porous medium for the column experiments.

Sodium persulfate ($Na_2S_2O_8$, 98+%) was obtained from Acros Organics. Hydrogen peroxide (H_2O_2, 35%) was obtained from Sigma-Aldrich. 1,4-dioxane ($C_4H_8O_2$) was from Fisher Scientific (Fair Lawn, NJ). 5,5-Dimethyl-1-pyrroline-N-oxide (DMPO, 98%) was from Matrix Scientific (Columbia, SC). All other chemicals used in this study were of reagent grade and used as received. The concentration of dioxane was 0.5 mM (44 mg/L) for all the experiments, which is representative of the upper range of groundwater concentrations reported for contaminated sites (Mohr et al., 2010). Concentrations of persulfate and H_2O_2 were 5 mM (1190 mg/L and 170 mg/L, respectively) for all experiments. While these oxidant concentrations are in excess compared to the concentration of dioxane, they are much lower than the concentrations typically used for standard field ISCO applications. These lower concentrations are employed to enhance cost effectiveness.

2.2. Batch Experiments

The degradation of dioxane by iron-filings-activated persulfate was measured in batch reactors. Solutions of 10 mM $Na_2S_2O_8$ and 1 mM dioxane were mixed 1:1 (v:v) in a glass flask. Iron filings were added to the mixture to yield a solid-liquid ratio of 1:10 (w/w). The

flask was sealed with parafilm and placed on a rotary shaker table at approximately 200 rpm at a room temperature of 30±1°C. Subsamples (2 ml) were collected over the course of the batch experiment in glass vials, and placed in an ice-water bath to quench further reaction. The samples were centrifuged for 1 minute to separate iron filing particles, and the supernatant was transferred to a glass tube, cooled to ~0°C in an ice-water bath, and immediately analyzed for the concentrations of dioxane, persulfate, sulfate, ferrous ion, total iron, and pH. Each subsample comprised only a very small portion of the total reactor volume (approximately 1%) and, therefore, the sampling process was assumed to have no significant impact on the solid-liquid ratio or the relevant reactions.

The batch experiments included several control treatments. The purpose of the first control was to determine dioxane degradation by persulfate in the absence of iron filings. For comparison purposes, dioxane degradation by H_2O_2 was also examined. The second control was to determine dioxane degradation in the presence of iron filings but absence of persulfate. Another set of controls was designed to determine separately the reactivity of persulfate and sulfate with the iron filings in the absence of dioxane. The final control, dioxane solution with no oxidant or iron filings, tested for loss of dioxane due to volatilization, photochemical decomposition, or other potential mass-loss processes during the course of the batch experiments.

Dioxane concentration was measured using gas chromatography (Shimadu GC-14A, Columbia, MD) equipped with a SPB™-624 capillary column (Supelco, 30m×0.53 mm×3μm) and a flame ionization detector. Splitless direct injection was used with injector temperature of 200°C. The temperature program was set to start at 40°C and then ramp to 110°C at 10°C/min. Detector temperature was 250°C. A modified iodide spectrophotometry method of Liang et al. (2008) was used to determine persulfate ($S_2O_8^{2-}$) and H_2O_2 concentrations. KI salt was dissolved in a 5 g/L $NaHCO_3$ solution to the concentration of 100 g/L. Samples were mixed with the KI-$NaHCO_3$ solution at a ratio of 1:19 (v:v). Absorptivity of the solution was measured after a 20 minute holding time with spectrophotometry (Hach DR2800, Loveland, CO) at a wavelength of 400 nm. Interference by ferric iron in solution on the absorptivity of the persulfate or H_2O_2 complex was corrected via independent analysis for the solution-phase concentration of ferric iron and associated relative absorptivity. Sulfate, ferrous ion, and total iron were measured with spectrophotometry using the Ba^{2+}-based USEPA SulfaVer4 method (HACH module No. 8051), 1,10-phenanthroline-based method (No. 8146), and FerroVer method (No. 8008), respectively. The ferric iron concentration was calculated as the difference between total iron and ferrous ion concentrations. The pH of the samples was measured by a Beckman 510 pH meter (Brea, CA).

2.3. Column Experiments

The columns used in the experiments were constructed of 316-stainless steel. They have a 2.2-cm inner diameter and are either 25-cm or 7-cm long. Porous frits were placed on each end of the column to promote uniform flow and retain the porous media. All tubing, frits, and connectors were constructed of stainless steel.

The 25-cm column was dry packed with a 20-cm length of iron filings, capped at each end with 2.5 cm of sand. The vertically oriented packed column was then flushed with CO_2 to displace air, and then saturated with deaerated water using a single-piston precision-flow HPLC pump (Gilson, Acuflow Series II). The column was then oriented horizontally for the experiments.

A solution of 5 mM persulfate or a mixed solution of 5 mM persulfate and 0.5 mM dioxane was injected into the column at a constant flow rate of either ~1 or ~0.1 ml/min, equivalent to pore-water velocities of ~30 or ~3 cm/h. After 7~9 pore volumes of injection, the influent was switched to water. Effluent samples were collected in glass tubes emplaced in an ice-water bath to quench the reaction, and weighed. The samples were then immediately analyzed for concentrations of dioxane, persulfate, sulfate, ferrous ion, total iron, and pH, accordingly. The concentrations of persulfate and dioxane in the reservoir were measured before, during, and after each experiment to monitor for potential loss.

Control experiments were conducted using identical procedures. One set of experiments was conducted to measure the potential reactivity of dioxane to the iron filings in the absence of persulfate. Another experiment was conducted to evaluate the transport and degradation of persulfate in silica sand. Finally, experiments were conducted with hydrogen peroxide as the oxidant in place of persulfate.

2.4. Ancillary Studies

Specific experiments were conducted to investigate the impact of combining persulfate and iron-filings on aqueous and solid-phase geochemistry. Iron filings (15 g) were added to flasks containing either 150 ml of 5 mM $Na_2S_2O_8$ solution or 150 ml of nano-pure water. The flasks were sealed with parafilm and shaken at 200 rpm (30±1°C). Subsamples (10 ml) were collected from the flasks at 1 h and 24 h, and analyzed for aqueous-phase concentration of persulfate, sulfate, Fe^{2+}, total iron, and pH following the procedures described above. Concentrations of metals in the subsamples were analyzed using inductively coupled plasma mass spectrometry (ICP-MS, ELAN DRC-II, Perkin Elmer, Shelton, CT). The calibration solution was prepared in 1% nitric acid from multi-element stock solutions such as those available from AccuStandard (New Haven, CT). Immediately after the 10-ml subsample was drawn from the flask, the remainder of the solution in the flask was discarded and the iron filings were rinsed more than 10 times with de-ionized water. The iron filings were then dried in pure N_2 atmosphere under room temperature. The dried iron filings were analyzed with electron scanning microscopy-energy dispersive X-ray spectroscopy (SEM-EDS, S-3400N SEM with UltraDry EDS, Thremo-scientific, Madison, WI) for surface element composition, and with X-ray diffraction (XRD, D8 Advance, Bruker AXS, Madison, WI) to identify minerals formed on the surface.

Formation of radicals was examined employing electron paramagnetic resonance spectroscopy. Two ml of the reaction solution (supernatant with suspended fine iron particles if iron filings were present) was mixed with the spin trapping agent DMPO to a final DMPO concentration of ~0.1 M. The mixed solution was immediately placed in capillaries with 1 mm ID, and analyzed with an X-band EPR spectrometer (Elexsys E500, Bruker, Woodlands, TX) equipped with the rectangular resonator operating in TE_{102} mode.

The spectra were recorded at room temperature, at the microwave frequency of 9.340 GHz, microwave power of 2 mW, and magnetic field modulation amplitude of 1 G.

3. RESULTS AND DISCUSSION

3.1. Batch Experiments

The surface chemistry of the iron filings was analyzed with SEM-EDS and XRD, and the results are presented in Table 1 and in Figure S1 in the Supplementary Information (SI). O, Fe, and C are the three major elements on the surface of the iron filings. Oxygen was introduced as the iron filings were oxidized by O_2 in the air. Carbon is a common element in the source steel. Low levels of silicon were identified, which is attributed to dust introduced during collection and transportation of the iron filings. A small quantity of manganese was also observed, likely due to its use as an additive for alloy steels. XRD results showed that magnetite with chemical formula of Fe_3O_4 is the major form of oxidized iron on the surface of the iron filings.

The results of the dioxane degradation batch experiments conducted in the absence of iron filings are presented in Figure 1. Dioxane loss for the control, due to volatilization, photochemical decomposition, or other processes, is minimal. This is consistent with the fact that dioxane has low vapor pressure at room temperature (~4.0 Kpa at 20°C; Verschueren, 1983) and is chemically stable under ambient conditions. In contrast, dioxane underwent significant degradation in the presence of persulfate (no iron filings) with an approximately 70% loss in the first 300 h. As the reaction proceeded, sulfate was detected and the concentration increased over time. The combined concentration of sulfate and persulfate was close to the initial persulfate concentration during the entire experiment, showing complete mass balance for sulfur and indicating that sulfate was the only measurable product of persulfate decomposition.

The reaction is assumed to follow first order kinetics given that the oxidant is present in great excess (molar ratio of oxidant to dioxane is 10:1). First-order reaction rate constants for dioxane and persulfate decomposition were calculated to be 0.006 (Table 2) and 0.00033 h^{-1} (Figure S2B, SI), respectively. By the end of the reaction, the molar decomposition ratio is calculated to be 0.5:1 (dioxane:persulfate) (Figure 1), indicating high efficiency for persulfate degradation of dioxane. In contrast, degradation of dioxane was minimal when H_2O_2 was used as the oxidant, with a first-order reaction rate constant of 0.0003 h^{-1} (Table 2). Approximately 35% of H_2O_2 was lost from solution after 300 h (Figure S2B, SI). This result shows that H_2O_2 is less efficient for dioxane degradation and has lower stability than persulfate.

The results of the dioxane degradation experiments conducted with the addition of iron filings are presented in Figure 2. There was approximately 10% loss of dioxane in the absence of persulfate (Figure 2A). This is in contrast to the no measurable loss observed for the control with no iron filings added. These contrasting results indicate that the iron filings apparently produced a small degree of dioxane degradation. Dioxane degradation in open aqueous systems in the presence of micron- (~44 μm) or nano-sized (~1 μm) particles of ZVI has been reported (Son et al., 2009; Shina et al., 2012). Such degradation was caused by

dissolved oxygen oxidation catalyzed by the ZVI. The pseudo-first-order reaction rate constants, *k*, vary from 0.03 to 0.18 h^{-1}, depending on the experimental setup, particle size, and solid-liquid ratio. The *k* for dioxane degradation with iron filings in this study is 0.0014 h^{-1} (Table 2). The significantly smaller value determined for our experiments is to be expected given the significantly greater reactive surface areas associated with the micron- or nano-ZVI compared to the iron-filing particles used herein.

Dioxane concentrations decreased rapidly in the presence of combined persulfate and iron filings, and approximately 70% of the dioxane was removed within 50 h (Figure 2A). Dioxane degradation was significantly faster in the presence of iron filings, wherein 70% reduction in dioxane required 300 hours in the absence of iron filings. Dioxane degradation exhibited a two-stage reaction pattern in the presence of iron filings. An extremely high reaction rate was observed in the first 0.5 h of contact, with 30% of dioxane removed. After 0.5 h, degradation of dioxane slowed and followed first-order kinetics with a *k* of 0.016 h^{-1} (Table 2 and Figure S2A, SI). Approximately 85% of the persulfate was lost from bulk solution within the first 0.5 h, resulting in production of a substantial amount of sulfate. This rapid loss of persulfate and concomitant production of sulfate contrasts greatly with the results observed for the experiment conducted without the iron filings (Figure 1). The results for dioxane, persulfate, and sulfate all demonstrate that the iron filings produced rapid activation of persulfate.

The concentration of total sulfur in bulk solution deceased after the reaction was initiated, and there was a loss of approximately 30% in total sulfur by the end of the experiment. Recall that there was no measurable loss of total sulfur for the experiment conducted with no iron filings present. Loss of sulfur from solution was also observed for the control tests wherein iron filings were added to sulfate (10 mM) or persulfate (5 mM) solutions with no dioxane present (Figure 2A). It is hypothesized that the sulfur loss observed for the iron-filings experiments is related to transfer of sulfur from bulk solution to the iron filings surface.

Enrichment of sulfur on the surface of the iron filings was observed with SEM-EDS after 1-h contact between iron filings and persulfate solution (Figure 3A and 3B). This sulfur species existed in a form that could not be removed by repeated flushing with deionized water, showing that it was bound in some manner to the iron filing surface. Consistent with the SEM-EDS observations, the XRD analysis indicated the presence of minerals in the form of $Fe_2(SO_4)_3$ and $FeSO_4$ on the iron filing surface after 1-h contact with persulfate. Enrichment of sulfur on the solid surface was not observed for the original iron filing sample or the control sample shaken with water for 24 h. In addition, after 24-h contact, the sulfur species associated with the iron filing surface observed for the 1-hr sample disappeared, which was accompanied with a decrease in the relative abundance of Fe (Figure 3B).

Solution pH increased for the batch experiment, which is expected due to consumption of persulfate, the source of H^+, in the presence of iron filings. Large amounts of both ferrous and ferric iron were released to the aqueous phase as a result of reaction between persulfate and iron filing surface (Figure 2B). The metals and their concentrations in bulk solution measured by ICP-MS are presented in Table S1, SI. Release of Fe was also observed by

ICP-MS and the concentration was close to the total Fe concentration measured spectrophotometrically. Soluble manganese with concentration higher than 5 mg/L was also detected. In contrast, contact of the iron filings with water (no persulfate) for 24 h had little impact on iron filing surface element composition and caused minimal release of metals (Table S1, SI).

3.2. Miscible-Displacement Experiments

Transport of persulfate in the column packed with sand was ideal, with no measurable retardation or mass loss (Figure S3, SI). In contrast, persulfate exhibited retardation (breakthrough at approximately 3 pore volumes) and significant mass loss (~85%) during transport in the iron filings (Figure 4A). Sulfate production was observed, with breakthrough occurring at approximately 1 pore volume, much earlier than persulfate (Figure 4A). This is because transformation of persulfate to sulfate was quick and adsorption of sulfate by iron filings was minimal, as indicated by the results of the batch experiment (Figure 2A). An initial plateau in sulfate concentration was observed at approximately C/C_0 of 0.55. A subsequent rise in sulfate concentration occurred coincident with persulfate breakthrough. The pH of the effluent was approximately 5.5 at the time of persulfate injection, increased to 9.5 for two pore volumes, and then returned to the initial value coincident with persulfate breakthrough. Significant increases in both ferrous and ferric iron were also observed coincident with persulfate breakthrough. This release of Fe to the aqueous phase was not a result of the decrease in pH, given that Fe concentrations were lower than 1 mg/L in the effluent at the beginning of injection when the pH was also initially lower.

Dioxane transport in the iron filing column was ideal in the absence of oxidants, with no retardation or mass loss (Figure S4, SI). The observed no mass loss for this column experiment, for which the hydraulic residence time (t_r) was approximately 7 h, is consistent with the results of the batch experiment wherein no loss of dioxane occurred within ~6 h after mixing with iron filings (Figure 2A). There was also minimal mass loss of dioxane in the presence of persulfate for the experiment conducted at the pore-water velocity of 31 cm/h (t_r = 0.6 h) (Figure 5A). However, the transport behavior of the sulfur species was essentially identical to that observed for the experiment conducted without dioxane (Figure 4A), indicating excellent reproducibility.

Approximately 10% of the dioxane injected was degraded when the pore-water velocity was lowered to 3 cm/h (t_r = 6.7 h) (Figure 5A). Patterns of iron species production and pH change in the effluent (Figure 5B) were similar to the experiment conducted without dioxane (Figure 4B). By assuming dioxane degradation follows first-order kinetics, a reaction rate constant k of 0.018 h^{-1} is obtained for pore-water velocity of 3 cm/h by solving the first-order kinetics equation:

$$C = C_0 e^{-kt_r} \quad (1)$$

$$t_r = L/v \quad (2)$$

$$v=4Q/(\pi \mathrm{D}^2 n) \quad (3)$$

where C (mM) is the mean dioxane concentration in the effluent at steady state, C_0 (mM) is the dioxane concentration in the influent, L (cm) is the length of the iron filing bed, v (cm/h) is the mean pore-water velocity, Q is flow rate (mL/h), D is the inner diameter of the column (cm), and n is porosity. The k determined from the column experiment is essentially identical to the k obtained for the second reaction stage of the batch experiment (0.016 h^{-1}).

When H_2O_2 was used in the column experiment, no breakthrough of H_2O_2 or degradation of dioxane was observed for either pore-water velocity (Figure S5A and S5C, SI). Release of ferrous or ferric ion into the bulk aqueous phase was minimal compared to the case of persulfate (two order of magnitude lower), and also no significant variation of pH was observed (Figure S5B and S5D, SI). The results are consistent with the fact that H_2O_2 is not stable and readily self-decomposes. These results suggest that persulfate is superior to H_2O_2 for oxidative removal of dioxane using iron-filing-based PRB.

3.3 Free Radical Analysis

The results obtained from the experiment conducted specifically to characterize free-radical formation are presented in Figure S6, SI. Both DMPO-OH and DMPO-SO_4 signals were observed in the EPR spectrum measured for the persulfate solution, which shows the presence of both $HO^{\bullet}$ and $SO_4^{\bullet -}$ radicals. This is consistent with prior observations (Fang et al., 2013; Yan et al., 2015). The DMPO-SO_4 signal diminished quickly over time, accompanied by a slight increase in the DMPO-OH signal, due to conversion of DMPO-SO_4 adduct to DMPO-OH (Davies et al., 1992; Zalibera et al., 2009; Yan et al., 2015).

The persulfate-dioxane solution with iron filings present exhibited a much more complicated EPR spectrum than the others (Figure 6A). Radicals other than $HO^{\bullet}$ and $SO_4^{\bullet -}$, such as a spin adduct with H (DMPO-H) and a carbon-centered radical (DMPO-R), were observed (Figure 6B). Such radicals could be intermediate radicals generated during decomposition of dioxane. The signal of these radicals diminished over time and the DMPO-OH signal intensity also decreased, as shown by repetitive scanning on the same sample for 30 min (Figure 6B).

The above results demonstrate that significant quantities of radicals are generated immediately upon combining persulfate and the iron filings. The very fast rate of dioxane degradation observed during the first 0.5 hour of the batch experiment is attributed to this surfeit of radicals in solution. However, the data presented in Figure 6B indicate that the concentration of radicals in solution decreases rapidly over 0.5 h. Additionally, EPR analysis of samples from the batch experiment shows that radical presence is minimal after 0.5 h (Figure S7, SI). This is consistent with the fact that the persulfate concentration decreased by 85% within 0.5 h (Figure 2), which thereby significantly reduced the source of radicals. The continued, albeit slower, degradation of dioxane in the absence of significant free-radical levels after 0.5 h indicates the existence of a second reaction process. This process is hypothesized to comprise a surface reaction mechanism. Such a mechanism is supported by the SEM-EDS and XRD results discussed above, which show a temporary accumulation of

sulfur species on the iron filings surface. This mechanism is also hypothesized to be responsible for the retardation of persulfate, two-stage increase in sulfate concentration, and significant release of iron to the aqueous phase observed for the column experiments.

4. Conclusion

Successful activation of persulfate was achieved by using iron filings in both batch and column experiments. The activation process comprises two stages, including a first stage of rapid decomposition of persulfate and a second stage of rate-limited surface reaction. Comparison of the pseudo-first-order reaction rate constants for dioxane degradation shows significantly higher reaction rates in the presence of iron filings, indicating the effectiveness of iron filing in activating persulfate and facilitating dioxane degradation.

The PRB bed length required for field application of the persulfate-enhanced PRB can be calculated based on assumed first-order reaction kinetics and using the reported k of 0.018 h^{-1}. Assuming the persulfate is perfused uniformly within the PRB, and given a typical groundwater velocity of 0.3 m/d, the estimated bed lengths (L in equation (2)) are 1.6, 2.1, and 3.2 m for dioxane removal rates of 90%, 95%, and 99% (C/C_0 = 0.1, 0.05, and 0.01), respectively. These thicknesses are in the range of bed lengths typically used for PRB applications. It is significant to note that the persulfate concentration used herein, ~1 g/L, is an order of magnitude lower than the concentrations typically used in standard field ISCO applications. It is also interesting to note that the k (0.018 h^{-1}) is comparable to the values (0.03~0.12 h^{-1}) obtained with micron- or nano-ZVI in batch experiments (Son et al., 2009; Shina et al., 2012), indicating that the persulfate-enhanced PRB has the potential to achieve a dioxane removal efficiency similar to nano-ZVI. These results illustrate the potential of the persulfate-enhanced PRB for in-situ remediation of dioxane contaminated groundwater.

Supplementary Material

Refer to Web version on PubMed Central for supplementary material.

Acknowledgments

The authors thank Andrei Astashkin in Department of Chemistry and Biochemistry, Paul Wallace in University Spectroscopy & Imaging Facility (USIF), Prakash Dhakal in Center for Environmental Physics and Mineralogy, and Mary Kay Amistadi in Arizona Laboratory for Emerging Contaminants (ALEC), University of Arizona, for their assistance on EPR, SEM-EDS, XRD, and ICP-MS analyses, respectively. The authors also thank the reviewers for constructive comments. This research is supported by the National Institute of Environmental Health Sciences Superfund Research Program (ES04940) and Strategic Environmental Research and Development Program (ER-2302).

References

Ahmad M, Teel AL, Watts RJ. Persulfate activation by subsurface minerals. J Contam Hydrol. 2010; 115:34–45. [PubMed: 20439128]

Anipsitakis GP, Dionysiou DD. Radical generation by the interaction of transition metals with common oxidants. Environ Sci Technol. 2004; 38:3705–3712. [PubMed: 15296324]

Block, PA.; Brown, RA.; Robinson, D. Novel Activation technologies for sodium persulfate in situ chemical oxidation. Proceedings of the Fourth International Conference on Remediation of Chlorinated and Recalcitrant Compounds; May 24–27, 2004; Monterey, CA. Columbus, OH, 2A-05: Battelle Press; 2004.

Buxton GV, Malone TN, Salmon GA. Reaction of $SO_4^{\bullet-}$ with Fe^{2+}, Mn^{2+} and Cu^{2+} in aqueous solution. J Chem Soc Faraday Trans. 1997; 93:2893–2897.

Davies MJ, Gilbert BC, Stell JK, Whitwood AC. Nucleophilic substitution reactions of spin adducts. Implications for the correct identification of reaction intermediates by EPR/spin trapping. J Chem Soc Perkin Trans. 1992; 2:333–335.

EPA. Treatment Technologies for 1, 4-Dioxane: Fundamentals and Field Applications. 2006

Fang GD, Dionysiou DD, Zhou DM, Wang Y, Zhu XD, Fan JX, Cang L, Wang YJ. Transformation of polychlorinated biphenyls by persulfate at ambient temperature. Chemosphere. 2013; 90:1573–1580. [PubMed: 22921645]

Fang GD, Gao J, Dionysiou DD, Liu C, Zhou DM. Activation of persulfate by quinones: free radical reactions and implication for the degradation of PCBs. Environ Sci Technol. 2013; 47:4605–4611. [PubMed: 23586773]

Furman OS, Teel AL, Watts RJ. Mechanism of Base Activation of Persulfate. Environ Sci Technol. 2010; 44:6423–6428. [PubMed: 20704244]

Ghauch A, Tuqan AM, Kibbi N. Ibuprofen removal by heated persulfate in aqueous solution: a kinetics study. Chem Eng J. 2012; 197:483–492.

Guan YH, Ma J, Li XC, Fang JY, Chen LW. Influence of pH on the formation of sulfate and hydroxyl radicals in the UV/peroxymonosulfate system. Environ Sci Technol. 2011; 45:9308–9314. [PubMed: 21999357]

Huang K, Zhao Z, Hoag G, Dahmani A, Block P. Degradation of volatile organic compounds with thermally activated persulfate oxidation. Chemosphere. 2005; 61:551–560. [PubMed: 16202809]

Johnson RL, Tratnyek PG, Johnson RO. Persulfate persistence under thermal activation conditions. Environ Sci Technol. 2008; 42:9350–9356. [PubMed: 19174915]

Lee YC, Lo SL, Chiueh PT, Chang DG. Efficient decomposition of perfluorocarboxylic acids in aqueous solution using microwave-induced persulfate. Water Res. 2009; 43:2811–2816. [PubMed: 19443010]

Lee YC, Lo SL, Chiueh PT, Liou YH, Chen ML. Microwave-hydrothermal decomposition of perfluorooctanoic acid in water by iron-activated persulfate oxidation. Water Res. 2010; 44:886–892. [PubMed: 19879622]

Lee YC, Lo SL, Kuo J, Lin YL. Persulfate oxidation of perfluorooctanoic acid under the temperatures of 20–40 °C. Chem Eng J. 2012; 198–199:27–32. [PubMed: 22422014]

Liang CJ, Bruell CJ. Thermally activated persulfate oxidation of trichloroethylene: experimental investigation of reaction orders. Ind Eng Chem Res. 2008; 47:2912–2918.

Liang CJ, Bruell CJ, Marley MC, Sperry KL. Thermally activated persulfate oxidation of trichloroethylene (TCE) and 1,1,1-Trichloroethane (TCA) in aqueous systems and soil slurries. Soil Sediment Contam. 2003; 12:207–228.

Liang CJ, Bruell CJ, Marley MC, Sperry KL. Persulfate oxidation for in situ remediation of TCE. II. Activated by chelated ferrous ion. Chemosphere. 2004; 55:1225–1233. [PubMed: 15081763]

Liang CJ, Guo YY. Remediation of diesel-contaminated soils using persulfate under alkaline condition. Water Air Soil Pollut. 2012; 223:4605–4614.

Liang CJ, Huang CF, Mohanty N, Kurakalva RM. A rapid spectrophotometric determination of persulfate anion in ISCO. Chemosphere. 2008; 73:1540–1543. [PubMed: 18922560]

Liang CJ, Lee IL. In situ iron activated persulfate oxidative fluid sparging treatment of TCE contamination - a proof of concept study. J Contam Hydrol. 2008; 100:91–100. [PubMed: 18649972]

Liang CJ, Wang ZS, Bruell CJ. Influence of pH on persulfate oxidation of TCE at ambient temperatures. Chemosphere. 2007; 66:106–113. [PubMed: 16814844]

Mohr, TKG. Environmental Investigation and Remediation: 1,4-dioxane and other solvent stabilizers. CRC Press; Boca Raton, FL:

Nadim F, Huang K, Dahmani A. Remediation of soil and ground water contaminated with PAH using heat and Fe(II)- EDTA catalyzed persulfate oxidation. Water, Air, Soil Pollut: Focus. 2006; 6:227–232.

NRC (National Research Council). Alternatives for Managing the Nation's Complex Contaminated Groundwater Sites. Wash., DC: 2013.

Oh SY, Kang SG, Chiu PC. Degradation of 2,4-dinitrotoluene by persulfate activated with zero-valent iron. Sci Total Environ. 2010; 408:3464–3468. [PubMed: 20471066]

Rastogi A, Al-Abed SR, Dionysiou DD. Sulfate radicals based ferrous peroxymonosulfate oxidative system for PCBs degradation in aqueous and sediment systems. Appl Catal B. 2009; 85 (3–4): 171–179.

Shina J, Lee YC, Ahn YH, Yang JW. 1,4-Dioxane degradation by oxidation and sonication in the presence of different-sized ZVI in open-air system. Desalin Water Treat. 2012; 50:102–114.

Son HS, Im JK, Zoh KD. A Fenton-like degradation mechanism for 1,4-dioxane using zero-valent iron (Fe^0) and UV light. Water Res. 2009; 43:1457–1463. [PubMed: 19131086]

Verschueren, K. Handbook of environmental data on organic chemicals. 2. Van Nostrand Reinhold Co; New York: 1983.

Wang CW, Liang CJ. Oxidative degradation of TMAH solution with UV persulfate activation. Chem Eng J. 2014; 254:472–478.

Yan N, Liu F, Xue Q, Brusseau ML, Liu YL, Wang JJ. Degradation of trichloroethene by siderite-catalyzed hydrogen peroxide and persulfate: Investigation of reaction mechanisms and degradation products. Chem Eng J. 2015; 274:61–68. [PubMed: 26236152]

Yuan S, Liao P, Alshawabkeh AN. Electrolytic manipulation of persulfate reactivity by iron electrodes for trichloroethylene degradation in groundwater. Environ Sci Technol. 2014; 48:656–663. [PubMed: 24328192]

Zalibera M, Rapta P, Staško A, Brindzová L, Brezová V. Thermal generation of stable spin trap adducts with super-hyperfine structure in their EPR spectra: An alternative EPR spin trapping assay for radical scavenging capacity determination in dimethylsulphoxide. Free Radic Res. 2009; 43:457–469. [PubMed: 19353392]

Author Manuscript

Author Manuscript

Author Manuscript

- Persulfate is activated by iron filings to degrade dioxane
- Dioxane may undergo a surface reaction mechanism in persulfate/iron-filings system
- Persulfate is superior to H_2O_2 for dioxane degradation
- Persulfate-enhanced permeable reactive barrier was successful in treating dioxane

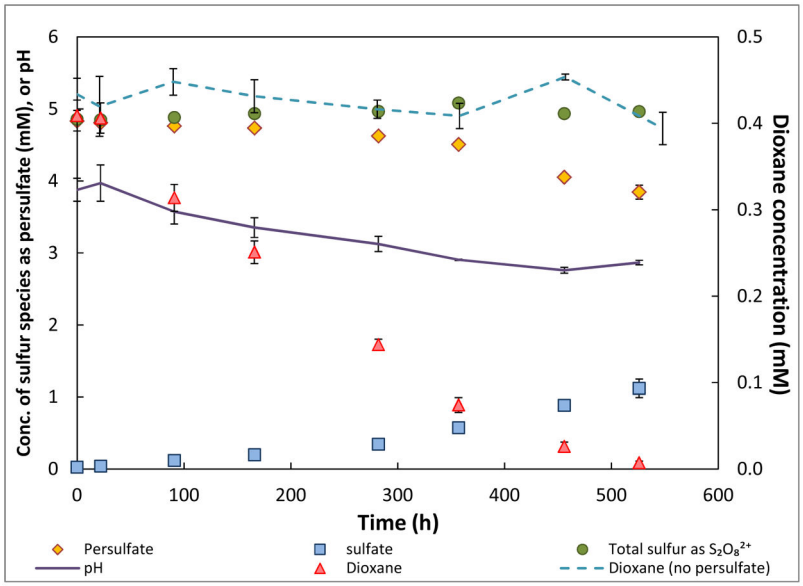

Figure 1.

Degradation of dioxane by persulfate in the absence of iron filings in batch reactor system. Error bars show mean ± standard deviation (range may be smaller than the symbol).

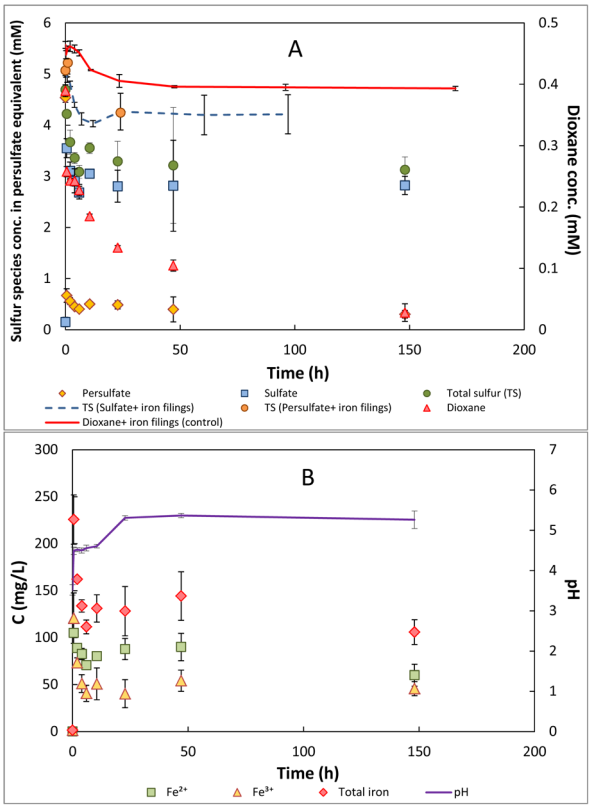

Figure 2.

Degradation of dioxane in the presence of iron filings in batch reactor system. Controls of persulfate + iron filings, sulfate + iron filings, and dioxane + iron filings are also included. (A) Concentration of sulfur species and dioxane versus time. (B) Concentration of iron species and pH versus time.

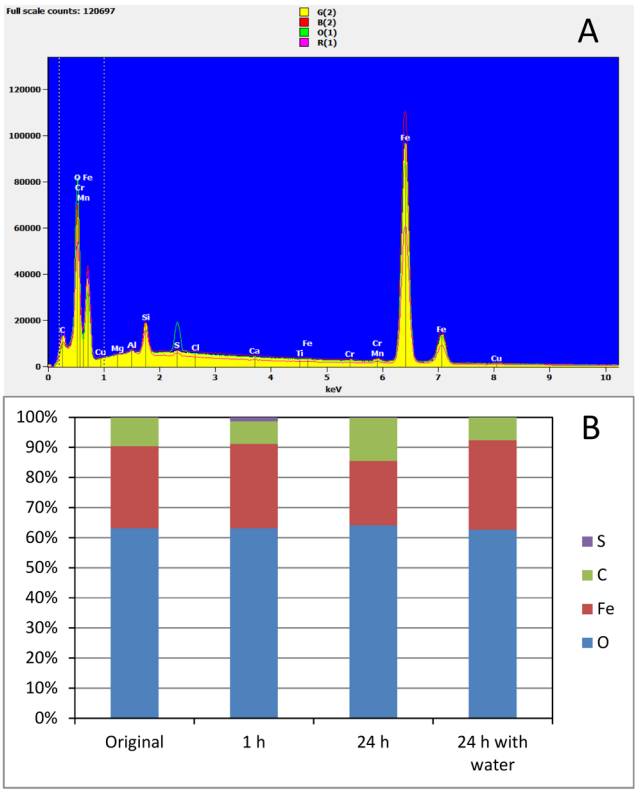

Figure 3.

Elements and their relative abundance on iron filing surface for activation of persulfate. (A) SEM-EDS spectra of the iron filing surface. G(2), original iron filings; O(1), after 1 h reaction; R(1), after 24 h reaction; B(2), after 24 h mixing with water. (B) Relative abundance of the four major elements on iron filing surface.

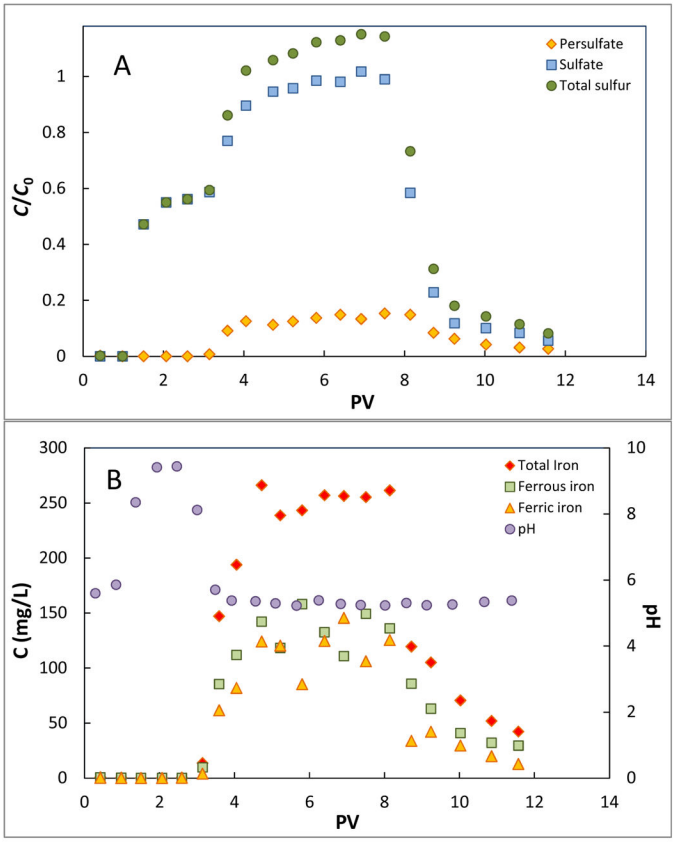

Figure 4.

Breakthrough curves of persulfate in iron filing column and the related solution chemistry (no dioxane present). Influent persulfate concentration is 5 mM. The pore-water velocity is 31 cm/h. (A) Breakthrough curves of persulfate, sulfate, and total sulfur. (B) Concentration of iron species and pH in the effluent.

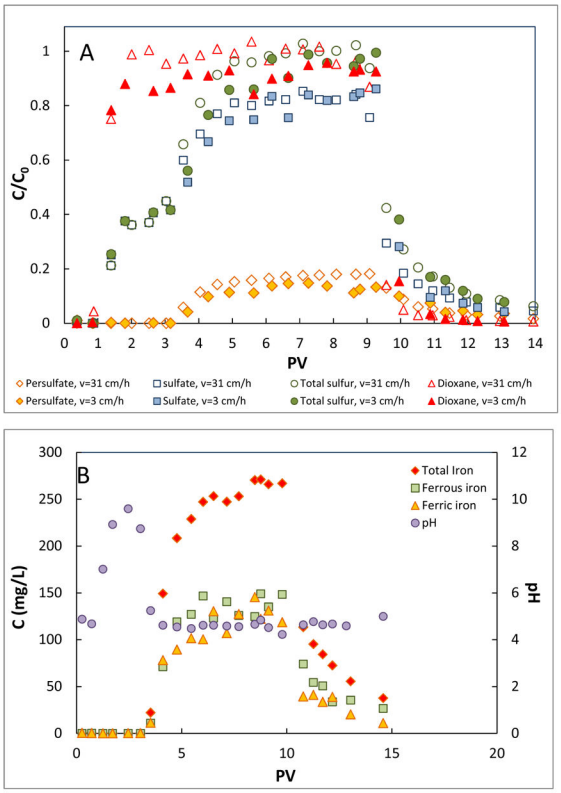

Figure 5.

Degradation of dioxane by persulfate in iron filing column and the related solution chemistry. Influent persulfate and dioxane concentrations are 5 mM and 0.5 mM, respectively. (A) Breakthrough curves of persulfate, sulfate, total sulfur and dioxane at pore-water velocities of 31 and 3 cm/h. (B) Concentration of iron species and pH in the effluent at the pore-water velocity of 3 cm/h.

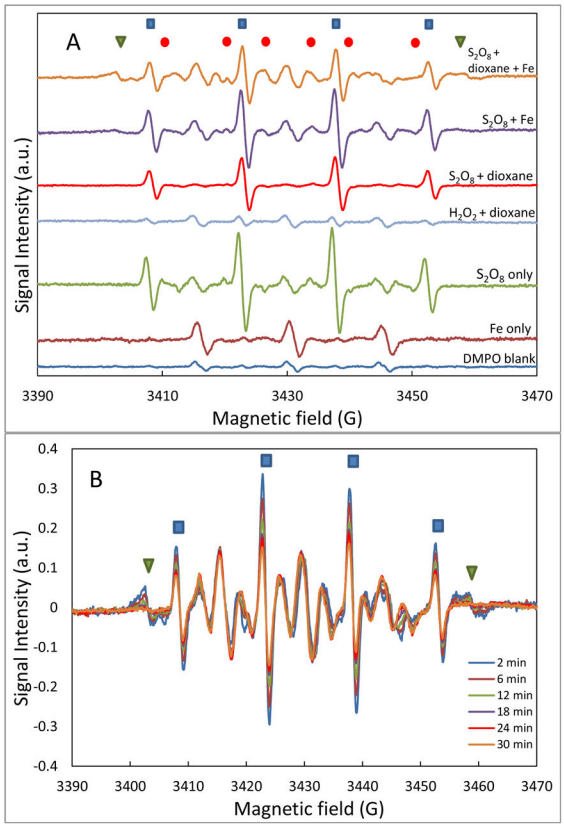

Figure 6.

Electron paramagnetic resonance (EPR) spectra. (A) EPR spectra for different reaction combinations at the start of reaction (~2 min). (B) EPR spectra versus time for supernatant of persulfate-dioxane-iron filing batch experiment. ■ DMPO-OH; ● DMPO-SO_4; ▼ DMPO-H or DMPO-R.

Table 1

Compounds and elements on surface of the iron filings based on XRD and SEM-EDS tests

Chemical name or formula	Mole Quantity (%)
Elements identified with SEM-EDS	
Oxygen (O)	61.97±0.28
Iron (Fe)	26.72±0.10
Carbon (C)	9.29±0.14
Silicon (Si)	1.06±0.02
Manganese (Mn)	0.37±0.04
Copper (Cu)	0.24±0.03
Sulfur (S)	0.12±0.01
Aluminum (Al)	0.09±0.01
Chromium (Cr)	0.09±0.01
Calcium (Ca)	0.05±0.01
Compounds identified with XRD	
Iron diiron(III) oxide, Magnetite (Fe_3O_4)	50
Iron titanium oxide ($Fe_{1.696}Ti_{0.228}O_3$)	26
Magnesium diiron(III) oxide ($MgFe_2O_4$)	17
Iron manganese(IV) oxide ($FeMnO_3$)	7

Table 2

Pseudo-first-order reaction rate constant k and half-life $t_{1/2}$ for dioxane degradation in batch experiments

Reactants	**Rate constant k (h^{-1})**	**Half-life $t_{1/2}$ (h)**
Dioxane only	0.00008	8664
Dioxane + H_2O_2	0.00029	2390
Dioxane + Fe filings	0.0014	495
Dioxane + persulfate	0.0060	116
Dioxane + persulfate + Fe filings[a]	0.016	43

[a] calculation is based on the data for the second reaction stage ($t \geq 0.5$ h, proposed surface reaction)